THE JOURNAL OF BIOLOGICAL CHEMISTRY VOL. 282, NO. 50, pp. 36403–36411, December 14, 2007
Printed in the U.S.A.

Metal-catalyzed Oxidation of the Werner Syndrome Protein Causes Loss of Catalytic Activities and Impaired Protein-Protein Interactions*

Received for publication, July 25, 2007, and in revised form, August 28, 2007 Published, JBC Papers in Press, October 2, 2007, DOI 10.1074/jbc.M706107200

Jeanine A. Harrigan[‡1], **Jason Piotrowski**[‡], **Luca Di Noto**[§], **Rodney L. Levine**[§], **and Vilhelm A. Bohr**[‡2]

From the [‡]*Laboratory of Molecular Gerontology, NIA, National Institutes of Health, Baltimore, Maryland 21224 and the* [§]*Laboratory of Biochemistry, NHLBI, National Institutes of Health, Bethesda, Maryland 20892*

Metal-catalyzed oxidation reactions target amino acids in the metal binding pocket of proteins. Such oxidation reactions generally result in either preferential degradation of the protein or accumulation of a catalytically inactive pool of protein with age. Consistently, levels of oxidized proteins have been shown to increase with age. The segmental, progeroid disorder Werner syndrome results from loss of the Werner syndrome protein (WRN). WRN is a member of the RecQ family of DNA helicases and possesses exonuclease and ATP-dependent helicase activities. Furthermore, each of the helicase and exonuclease domains of WRN contains a metal binding pocket. In this report we examined for metal-catalyzed oxidation of WRN in the presence of iron or copper. We found that WRN was oxidized *in vitro* by iron but not by copper. Iron-mediated oxidation resulted in the inhibition of both WRN helicase and exonuclease activities. Oxidation of WRN also inhibited binding to several known protein partners. In addition, we did not observe degradation of oxidized WRN by the 20 S proteasome *in vitro*. Finally, exposure of cells to hydrogen peroxide resulted in oxidation of WRN *in vivo*. Therefore, our results demonstrate that WRN undergoes metal-catalyzed oxidation in the presence of iron, and iron-mediated oxidation of WRN likely results in the accumulation of a catalytically inactive form of the protein, which may contribute to age-related phenotypes.

Many age-related changes are proposed to be a consequence of oxidative damage. Reactive oxygen species react with all three of the major cellular macromolecules: nucleic acids, lipids, and proteins. Many of the reactions mediated by reactive oxygen species result in the introduction of carbonyl groups to amino acid side chains in the protein, and the steady-state level of carbonyl-containing proteins increases exponentially during the last third of animal life spans (1), so that half of all proteins may become oxidized in an 80-year-old human (2). Within the protein, either the peptide or the side chain may be targeted. The protein may be cleaved to yield lower molecular weight products, or it may be cross-linked to give higher molecular weight species (1). These reactions are frequently influenced by redox cycling metal cations, especially iron or copper.

Both copper and iron are ubiquitous metals within the cell and are present in many enzymes and proteins. As transition elements, their ionic forms are prone to one-electron transfer reactions and thus enable iron and copper to generate radical species (3). For example, copper and iron participate in the Fenton reaction, in which the very reactive hydroxyl radical is generated. Compared with copper, the abundance of iron and the availability of loosely bound iron makes it the more likely source of hydroxyl radicals in biological systems (4, 5). Metal-catalyzed oxidation is a site-specific process in which only one or a few amino acids in the metal binding site of a protein are preferentially oxidized (6). For example, kinases and other nucleotide-binding proteins with manganese or magnesium requirements are predictably oxidized in a site-specific fashion (7). As with low molecular weight chelators, iron and copper bind to divalent cation sites with an affinity that is orders of magnitude greater than manganese or magnesium, thus explaining why even submicromolar concentrations of iron or copper can out-compete magnesium or manganese (8). The biological significance of metal-catalyzed oxidation reactions is that oxidatively modified proteins are often targeted for degradation, and failure to remove the modified proteins creates an intracellular pool of catalytically inactive or less active proteins, such as occurs with age (6).

Werner syndrome is a disorder characterized by premature aging. Werner syndrome patients appear much older than their chronological age and display many clinical features of normal aging, including cataracts, graying and thinning of the hair, type II diabetes, atherosclerosis, osteoporosis, and an increased incidence of sarcomas (9). Consistent with an aging phenotype, cells from Werner syndrome patients also have elevated levels of oxidized proteins (10). The gene mutated in Werner syndrome encodes a 1432-amino acid protein, WRN (Werner syndrome protein),[3] belonging to the human RecQ family of DNA helicases. Specifically, RecQ members belong to the SF2 superfamily of helicases, which contain a set of seven conserved

* This work was supported by the intramural research program of the National Institutes of Health (NIA and the NHLBI). The costs of publication of this article were defrayed in part by the payment of page charges. This article must therefore be hereby marked "*advertisement*" in accordance with 18 U.S.C. Section 1734 solely to indicate this fact.

[1] Present address: The Wellcome Trust/CRUK Gurdon Inst., University of Cambridge, Cambridge, CB2 1QN, UK.

[2] To whom correspondence should be addressed: Laboratory of Molecular Gerontology, NIA, National Institutes of Health, 5600 Nathan Shock Dr., Baltimore, MD 21224. Tel.: 410-558-8162; Fax: 410-558-8157; E-mail: vbohr@nih.gov.

[3] The abbreviations used are: WRN, Werner syndrome protein; TRF2, telomere repeat-binding factor 2; DNP, dinitrophenyl; DTT, dithiothreitol; Ku, Ku70/Ku80 heterodimer; PARP-1, poly(ADP-ribose) polymerase 1; PBS, phosphate-buffered saline; BSA, bovine serum albumin.

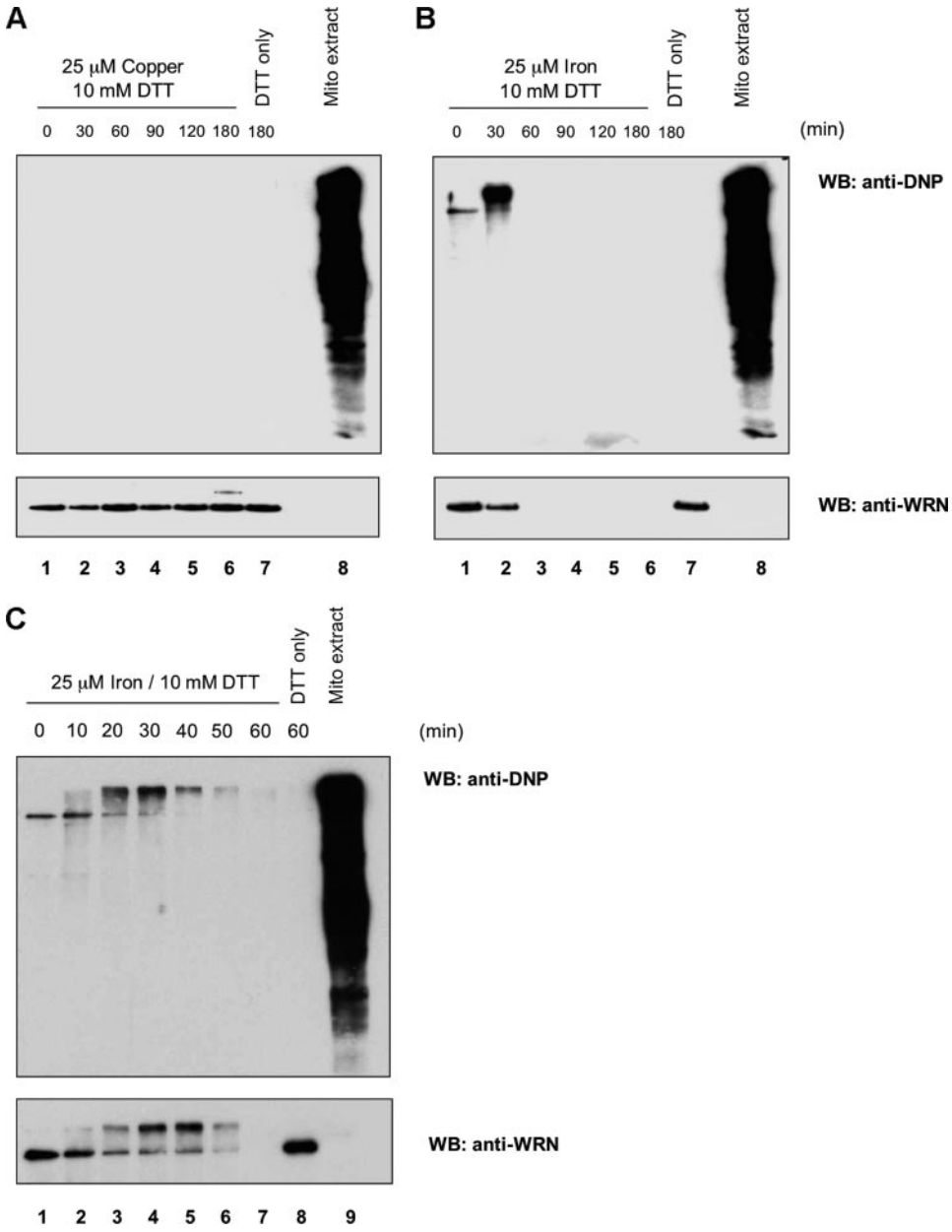

FIGURE 1. **WRN is oxidized *in vitro* by iron but not by copper.** *A*, recombinant WRN was incubated with 10 mM DTT in the absence (*lane 7*) or presence (*lanes 1–6*) of 25 μM copper at 37 °C for 0–180 min as indicated. Samples were run on SDS-PAGE, transferred to a polyvinylidene difluoride membrane, and blotted with anti-DNP antibodies (*upper panel*). Membranes were stripped and reprobed with anti-WRN antibodies (*lower panel*). Mitochondrial extracts (*lane 8*) were loaded on the gel as a positive control for oxidized proteins (anti-DNP). *B*, samples were treated as in *A*, except that WRN was incubated in the absence (*lane 7*) or presence (*lanes 1–6*) of 25 μM iron. *C*, samples were treated as in *B*, except that WRN was incubated in the absence (*lane 8*) or presence (*lanes 1–7*) of 25 μM iron for 0–60 min as indicated. *Lane 9*, mitochondrial extracts. *WB*, Western blot.

motifs (11, 12). Motifs I and II (Walker A and B boxes) contain amino acid residues important for ATP and metal binding (13). In addition to ATP-dependent helicase activity, WRN is unique among human RecQ family members in that it also possesses exonuclease activity. The exonuclease domain comprises three motifs (Exo I, Exo II, and Exo III) characteristic of the RNase D family of DNA proofreading enzymes (14). A protease-resistant core exonuclease domain (amino acids 38–236) of WRN was recently crystallized (15). The crystal structure reveals that two metal ions are bound in the active site (15), consistent with previously published alignments (14, 16). In fact, the metal binding pocket of the WRN exonuclease domain is able to accommodate two magnesium (Mg^{2+}), two manganese (Mn^{2+}), or two lanthanide (Eu^{3+}) ions (15).

WRN requires divalent metals for catalytic activity, and metal-catalyzed oxidation usually impairs or abolishes the catalytic activity of enzymes (7). Thus, oxidative modification of WRN would likely impair both helicase and exonuclease activities. Because the cellular accumulation of oxidatively modified proteins increases during aging (1) the net result would be a decrease in WRN activity, which could contribute to the aging phenotype. We therefore examined the susceptibility of WRN to metal-catalyzed oxidation and then the ability of oxidatively modified WRN to function catalytically, to interact with other proteins, as well as its susceptibility to degradation by the proteasome.

EXPERIMENTAL PROCEDURES

Materials—Synthetic oligonucleotides were purchased from Midland Certified Reagent Co. Cupric chloride (copper, Cu^{2+}) and ferric chloride (iron, Fe^{3+}) were from Sigma. Recombinant human WRN was purified as described previously (17), except that bovine serum albumin (BSA) and glycerol were omitted from the final storage buffer. Recombinant human TRF2 (telomere repeat binding factor 2) was purified as described previously (18). The Ku70/Ku80 heterodimer (Ku) was a gift from Dr. Dale Ramsden (Chapel Hill, NC) and poly(ADP-ribose) polymerase 1 (PARP-1) was a gift from Dr. Gilbert de Murcia (Strasbourg, France). The 20 S proteasome was purified from rat liver and assayed as described (19).

Protein Oxidation Reactions—Purified recombinant WRN (500 ng) was incubated in oxidation buffer (50 mM HEPES (pH 7.4), 100 mM KCl, 10 mM $MgCl_2$, and 10 mM dithiothreitol (DTT)) in the absence or presence of iron (2–50 μM) or copper (2–50 μM, Fig. 1 only) in a final volume of 20 μl for 30 min at 37 °C. Reactions were terminated by the addition of 2 μl of 22 mM EDTA (2 mM final). Oxidized WRN was then used for determination of carbonyl content or enzymatic activity assays as described below.

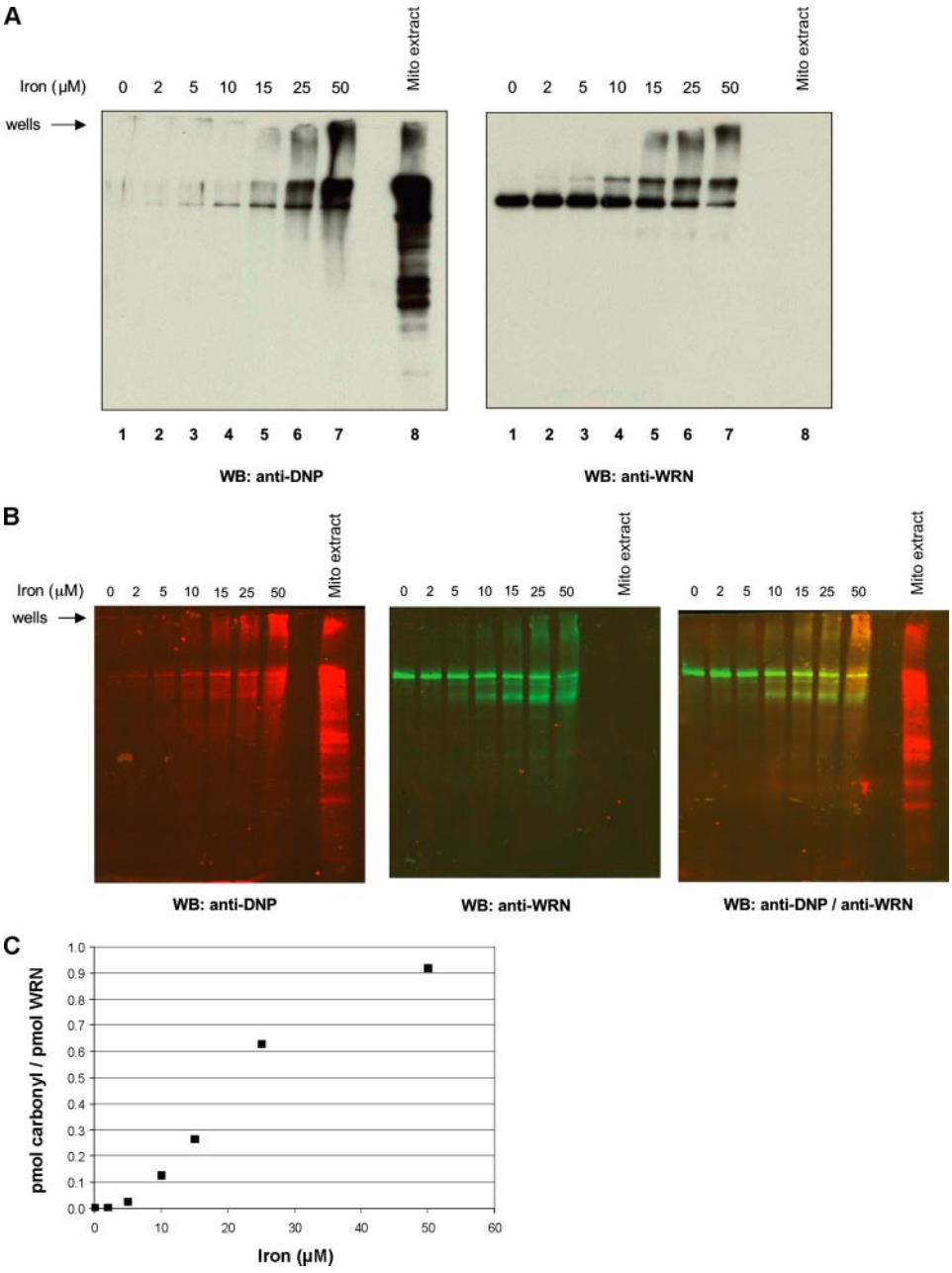

FIGURE 2. **Effect of iron concentration on metal-catalyzed oxidation of WRN.** *A*, recombinant WRN was incubated for 20 min at 37 °C with 10 mM DTT in the absence (*lane 1*) or presence (*lanes 2–7*) of increasing concentrations of iron as indicated. Samples were run on SDS-PAGE, transferred to a polyvinylidene difluoride membrane, and blotted with anti-DNP antibodies (*left panel*). Membranes were stripped and reprobed with anti-WRN antibodies (*right panel*). *Lane 8*, mitochondrial extracts. *B*, samples treated as in *A* were probed with anti-DNP (*left panel*), anti-WRN (*middle panel*), or both anti-DNP and anti-WRN antibodies (*right panel*). Membranes were then incubated with fluorescent secondary antibodies. *C*, corresponding signals from *B* were analyzed using the Odyssey infrared imager and associated software and quantitated as described under "Experimental Procedures." The average of two independent experiments is shown. *WB*, Western blot.

Protein Carbonyl Detection—Protein carbonyl groups were detected using the OxyBlot protein oxidation detection kit (Intergen, now Millipore) according to the manufacturer's instructions. Briefly, aliquots (5 μl) from protein oxidation reactions (~115 ng of WRN) were incubated with 12% SDS (5 μl) and 2,4-dinitrophenylhydrazine (10 μl) for 15 min at room temperature. Subsequently, neutralization solution (7.5 μl) was added. Alternatively, 5 μl of mitochondrial extract (1 μg/μl) was derivatized as described above. Samples were then analyzed by Western blotting.

Western Blotting—Proteins were separated by SDS-PAGE (10%) and transferred onto a polyvinylidene difluoride membrane (Bio-Rad). After blocking with 2.5% nonfat milk in phosphate-buffered saline containing 0.1% Tween 20 (PBS-T) for 1 h at room temperature, the membrane was incubated overnight at 4 °C with rabbit anti-dinitrophenyl (DNP) antibodies (Dako, 1:1000). After washing with PBS-T, the membrane was incubated with the corresponding horseradish peroxidase-conjugated secondary antibodies (Vector Laboratories, 1:10,000) for 1 h at room temperature. Antigen-antibody complexes were detected by enhanced chemiluminescence using ECL Plus (Amersham Biosciences). Membranes were stripped (62.5 mM Tris (pH 6.8), 2% SDS, and 100 mM 2-mercaptoethanol for 30 min at 50 °C) and reprobed with mouse anti-WRN antibodies (BD Biosciences, 1:250).

For quantitative immunodetection, polyvinylidene difluoride membranes were blocked for 1 h at room temperature with Odyssey blocking buffer (LI-COR Biosciences) and incubated overnight at 4 °C with rabbit anti-DNP antibodies (Dako, 1:2000), mouse anti-WRN antibodies (BD Biosciences, 1:400), or anti-DNP and anti-WRN antibodies. After washing with PBS-T, we employed either Alexa Fluor 680 goat anti-rabbit (Invitrogen, 1:10,000) or IRDye 800 goat anti-mouse (LI-COR Biosciences, 1:10,000) secondary antibodies labeled with dyes that fluoresce in the infrared region. Fluorescence was measured with an infrared laser imager (Odyssey, LI-COR Biosciences). Unoxidized WRN served as the protein standard and oxidatively modified glutamine synthetase with known carbonyl content served as the carbonyl standard (20).

Immunoprecipitation Assays—HeLa cells were pretreated for 1 h in the absence or presence of MG-132 (20 μM) in serum-free medium (Dulbecco's modified Eagle's medium containing only glutamine, penicillin, and streptomycin). Subsequently, cells were incubated in the absence or presence of 250 μM hydrogen

peroxide (H_2O_2) for an additional hour. Cells were washed twice with ice-cold PBS, scraped, and pelleted. Whole cell extracts were prepared by incubating cells in lysis buffer (50 mM Tris (pH 7.4), 150 mM NaCl, 1 mM diethylene triamine pentaacetic acid, 1% Nonidet P-40, 10 mM DTT, 1 mM phenylmethylsulfonyl fluoride, and 1 μg/ml pepstatin, aprotinin, and leupeptin) for 30 min on ice. Lysates were centrifuged at 15,000 $\times$ *g* for 20 min at 4 °C. Supernatants were precleared with protein A-Sepharose beads for 10 min at 4 °C. Extracts were incubated with either rabbit anti-WRN (H-300, Santa Cruz Biotechnology) or rabbit IgG (Santa Cruz Biotechnology) overnight at 4 °C. Protein A-Sepharose was added to each sample and incubated for 2 h at 4 °C. Samples were centrifuged and washed four times with lysis buffer. Bound proteins were derivatized as described above except that 10 μl of 12% SDS, 20 μl of 2,4-dinitrophenylhydrazine, and 15 μl of neutralization solution were used. Samples were eluted by boiling for 5 min and analyzed by SDS-PAGE and Western blotting using mouse anti-WRN antibodies (BD Biosciences, 1:250) or goat anti-DNP antibodies (Sigma, 1:500).

Helicase Assays—Oligonucleotide 22Fork 3 (5′-TTTTTTTTTTTTTTTGAGTGTGGTGTACATGCACTAC-3′) was 5′-end-labeled with [γ-^{32}P]ATP and T4 polynucleotide kinase (New England Biolabs) and annealed to its complementary strand, 22Fork 4 (5′-GTAGTGCATGTACACCACACTCTTTTTTTTTTTTTTTT-3′). Reactions (20 μl) were performed in helicase reaction buffer (40 mM Tris (pH 8), 10 mM $MgCl_2$, 5 mM DTT, and 0.1 μg/μl BSA) and contained DNA substrate (50 fmol), 2 mM ATP, and WRN (1.5 μl of a 1:10 dilution from the oxidation reaction as described above). Samples were incubated for 15 min at 37 °C and terminated by the addition of stop dye (16 mM EDTA, 0.3% SDS, 13% glycerol, 0.05% xylene cyanol, and 0.05% bromphenol blue). Reaction products were run

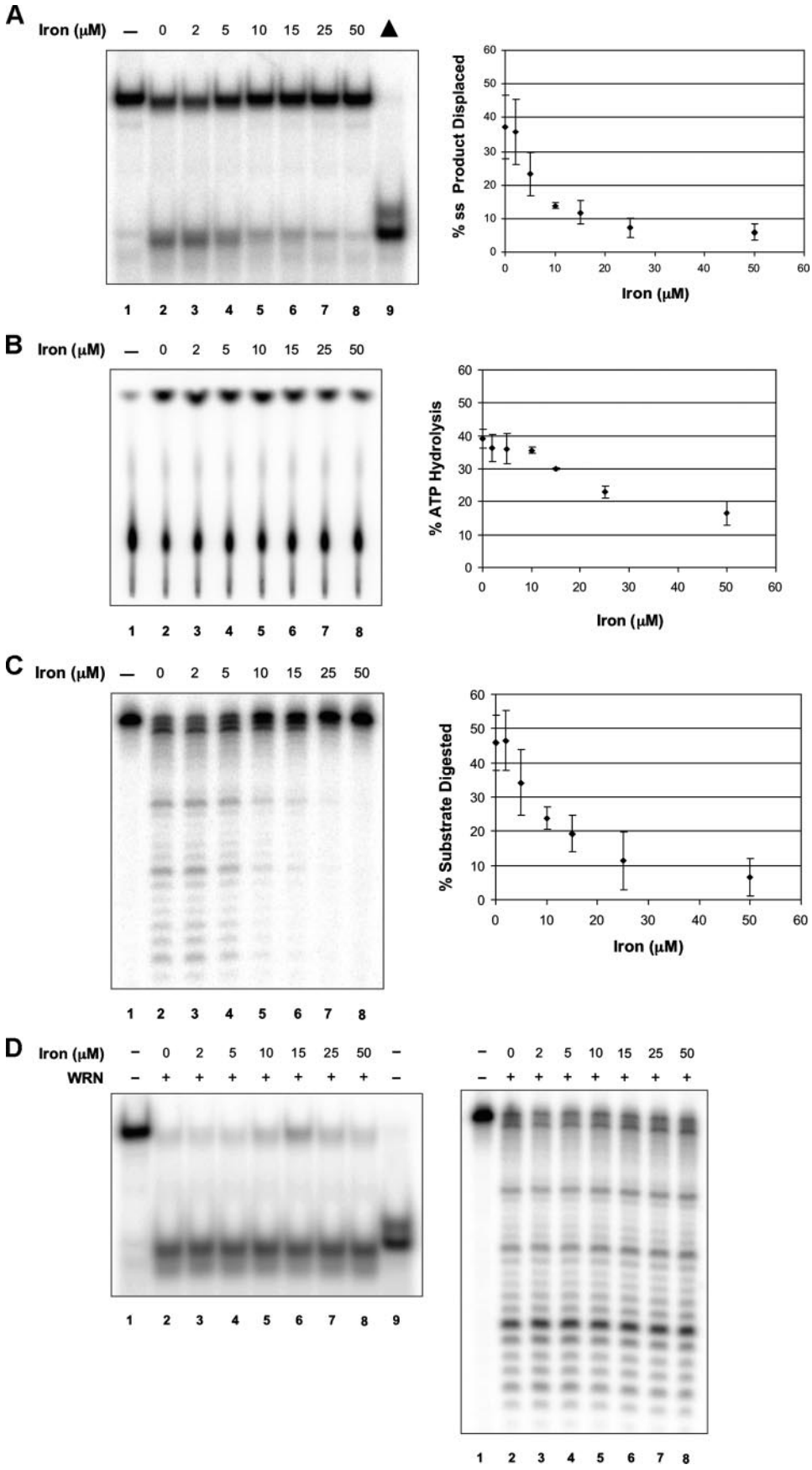

on a 12% nondenaturing polyacrylamide gel, visualized using a PhosphorImager, and quantitated using ImageQuant software.

ATPase Assays—ATPase reactions (10 μl) were performed in helicase reaction buffer containing M13mp18 DNA cofactor (150 ng), [γ-^{32}P]ATP (1 μCi), ATP (50 μM), and WRN (2 μl from the oxidation reaction described above, 279 fmol of WRN). Reactions were incubated for 30 min at 37 °C and terminated by the addition of 5 μl of 0.5 M EDTA. Samples were separated on a polyethylenimine/cellulose thin layer chromatography plate (Mallinckrodt Baker, Inc.) and developed in 1 M formic acid/0.8 M LiCl. Radioactive products were visualized using a PhosphorImager and quantitated using ImageQuant software.

Exonuclease Assays—Oligonucleotide 34Fork A (5′-TTTTTTTTTTTTTTTAGGGTTAGGGTTAGGGTTAGGGCATGCACTAC-3′) was 5′-end-labeled with [γ-^{32}P]ATP and T4 polynucleotide kinase (New England Biolabs) and annealed to its complementary strand 34Fork B (5′-GTAGTGCATGCCCTAACCCTAACCCTAACCCTAATTTTTTTTTTTTTTT-3′). Exonuclease reactions (10 μl) were performed in helicase reaction buffer containing DNA substrate (25 fmol), 2 mM ATP, and WRN (2 μl of a 1:10 dilution from the oxidation reaction described above). Samples were incubated for 15 min at 37 °C and terminated by the addition of formamide stop dye (80% formamide, 0.5× Tris borate-EDTA buffer, 0.1% xylene cyanol, and 0.1% bromphenol blue). Reaction products were heat denatured for 5 min at 95 °C, run on a 14% denaturing polyacrylamide gel, visualized using a PhosphorImager, and quantitated using ImageQuant software.

Enzyme-linked Immunosorbent Assay—The enzyme-linked immunosorbent assay was performed as described previously (21). Briefly, 500 fmol of Ku, PARP-1, or TRF2 was diluted in carbonate buffer and coated onto wells overnight at 4 °C. Wells were washed and incubated with blocking buffer (PBS, 2% BSA, and 0.1% Tween 20) for 1 h at 37 °C. Aliquots (3.5 μl, 500 fmol of WRN) from oxidation reactions were then added to the corresponding wells in a buffer containing PBS, 2% BSA, and 0.1% Tween 20 and incubated for 90 min at 37 °C. Wells were incubated with rabbit anti-WRN antibodies (Novus Biologicals, 1:1000) for 1 h at 37 °C followed by anti-rabbit secondary antibodies (Vector Laboratories, 1:10,000) for 1 h at 37 °C. Bound WRN was detected with *o*-phenylenediamine dihydrochloride followed by termination with 3 M H_2SO_4. Absorbance was read at 490 nm.

RESULTS

We first determined whether WRN underwent metal-catalyzed oxidation *in vitro*. We incubated purified recombinant WRN and DTT in the absence or presence of 25 μM copper or iron for up to 180 min. As shown in Fig. 1, WRN was not oxidized by copper during a 180-min incubation period (Fig. 1*A*, *upper panel*, *lanes 2–6*). Mitochondrial extracts served as a positive control for protein carbonyls (Fig. 1*A*, *lane 8*). Membranes were then stripped and reprobed with anti-WRN antibodies. Full-length WRN was observed in all lanes (Fig. 1*A*, *lower panel*, *lanes 1–7*). In addition, a slower migrating band was observed after a 180-min incubation in the presence of copper and DTT, indicative of protein cross-links or aggregates resulting from protein oxidation (Fig. 1*A*, *lower panel*, *lane 6*). However, as mentioned above, no signal was observed with anti-carbonyl antibodies (Fig. 1*A*, *upper panel*, *lane 6*), suggesting a limited amount of carbonyl groups or other forms of oxidation. In contrast to the results observed with copper, we observed a strong anti-carbonyl signal after incubation of WRN with iron and DTT for 30 min (Fig. 1*B*, *upper panel*, *lane 2*). Notably, the anti-carbonyl signal shifted to a higher molecular weight compared with the 0-min time point (Fig. 1*B*, *upper panel*, compare *lanes 1* and *2*). The anti-carbonyl signal was lost with longer incubation times (Fig. 1*B*, *upper panel*, *lanes 3–6*), which also corresponded to a loss of WRN protein (*lower panel*, *lanes 3–6*). The loss of WRN required iron, as WRN was observed in the presence of DTT alone after 180 min (Fig. 1*B*, *lower panel*, *lane 7*). Extensive oxidative modification of proteins is known to cause aggregation (Fig. 1*C*), which can eventually yield proteins that are SDS-insoluble (1) and explain the loss of WRN observed here. Because metal-catalyzed oxidation of WRN occurred within 30 min, but loss of WRN occurred at 60 min, we next took samples every 10 min over a 60-min time period. As shown in Fig. 1*C*, the anti-carbonyl signal increased at 10 min (*upper panel*, *lane 2*, note smear), was maximal after 30 min (*upper panel*, *lane 4*), and began to decrease by 40 min (*upper panel*, *lane 5*). WRN again shifted to a higher molecular weight product with incubation times between 10 and 40 min, with a maximal signal and shift at 30 and 40 min (Fig. 1*C*, *lower panel*). Thus, WRN undergoes iron-mediated metal-catalyzed oxidation.

We next investigated the effect of iron concentration on the metal-catalyzed oxidation. WRN was incubated with 0–50 μM iron in the presence of DTT. As shown in Fig. 2*A*, increasing

FIGURE 3. **Oxidation of WRN inhibits its catalytic activities.** *A*, purified recombinant WRN was incubated in the absence or presence of iron (0–50 μM) for 30 min at 37 °C. Subsequently, aliquots (containing 21 fmol of WRN) were taken from each reaction and incubated with a radiolabeled forked duplex substrate (Fork 3/4, 50 fmol) for 15 min at 37 °C. Reaction products were separated on a 12% native gel and visualized using a PhosphorImager. *Lane 1*, substrate alone. *Lane 9*, heat-denatured substrate. Quantitation (mean ± S.D.) of four independent experiments is shown in the *right panel*. *B*, oxidation reactions were performed as in *A*, and aliquots (containing 279 fmol of WRN) from each reaction were incubated with M13mp18 DNA cofactor and radiolabeled ATP for 15 min at 37 °C. Reaction products were separated by thin layer chromatography and visualized using a PhosphorImager. *Lane 1*, DNA cofactor and radiolabeled ATP only. Quantitation (mean ± S.D.) of three independent experiments is shown in the *right panel*. *C*, oxidation reactions were performed as in *A*, and aliquots (containing 28 fmol of WRN) from each reaction were incubated with a radiolabeled forked duplex substrate (Fork A/B, 25 fmol) for 15 min at 37 °C. Reaction products were separated on a 14% denaturing gel and visualized using a PhosphorImager. *Lane 1*, substrate alone. Quantitation (mean ± S.D.) of four independent experiments is shown in the *right panel*. *D*, oxidation reactions were performed as in *A*, except purified recombinant WRN was omitted. Aliquots from each reaction were incubated for 15 min at 37 °C with a radiolabeled forked duplex substrate (Fork 3/4, 50 fmol) and 21 fmol of WRN as indicated for helicase reactions (*left panel*) or with a radiolabeled forked duplex substrate (Fork A/B, 25 fmol) and 31 fmol of WRN as indicated for exonuclease reactions (*right panel*). Helicase and exonuclease reaction products were analyzed as described in *A* and *C*, respectively. *Left panel*: *lane 1*, substrate alone; *lane 9*, heat-denatured substrate. *Right panel*: *lane 1*, substrate alone.

iron resulted in an increase in protein carbonyl in full-length WRN as well as higher molecular weight species detected with anti-carbonyl antibodies (*left panel*). Consistently, increasing iron resulted in a decrease in the full-length WRN form and an increase in shifted products (Fig. 2*A*, *right panel*). In addition, we incubated membranes either individually or simultaneously with anti-WRN and anti-carbonyl antibodies followed by incubation with fluorescent secondary antibody (Fig. 2*B*), allowing quantitation of protein carbonyl in WRN (Fig. 2*C*). Incubation with 50 μM iron resulted in ~1 carbonyl group per WRN molecule. As protein carbonyls are only one measurement of protein oxidation, our results likely underestimate the extent of WRN oxidation.

Metal-catalyzed oxidation within proteins is a caged free radical reaction that oxidizes amino acids at or near the metal binding pocket. As WRN contains metal binding pockets that are critical for catalytic activities, we next explored whether oxidation affects WRN helicase, ATPase, or exonuclease activities. WRN possesses seven conserved helicase motifs, which reside in the central portion of the protein (amino acids 545–740). The crystal structure of *Escherichia coli* RecQ shows a metal ion in the predicted ATP binding site in which the ion makes contacts with Ser-54 and Asp-146 of motifs I and II, respectively (22). To investigate the effects of metal-catalyzed oxidation on WRN helicase activity, we incubated recombinant WRN in the absence or presence of iron, terminated the oxidation reaction with EDTA, and subsequently performed unwinding assays. We observed that metal-catalyzed oxidation of WRN caused loss of helicase activity (Fig. 3*A*). Incubation of WRN with 10 or 25 μM iron inhibited WRN helicase activity 61 and 78%, respectively (Fig. 3*A*, *right panel*). As WRN helicase activity requires ATP hydrolysis, we next quantitated WRN ATPase activity following oxidation in the presence of iron. In contrast to the helicase assays, oxidation of WRN did not have as great an inhibitory effect on ATPase activity (Fig. 3*B*). Incubation of WRN with 10 and 25 μM iron inhibited WRN ATPase activity 9 and 41%, respectively (Fig. 3*B*, *right panel*). We next determined the effect of WRN exonuclease activity following metal-catalyzed oxidation in the presence of iron. The three exonuclease domains of WRN reside in the N terminus of the protein and the active site contains two metal ions (15). Similar to what was observed with WRN helicase assays, oxidation inhibited WRN exonuclease activity 46 and 72% in the presence of 10 and 25 μM iron, respectively (Fig. 3*C*, *right panel*).

We added EDTA to stop reactive oxygen species generation after oxidation of WRN, but some reactive oxygen species might still have been produced during the subsequent enzyme assay. If so, they could oxidize the DNA, which was added as a substrate, and oxidized DNA has been shown to inhibit WRN exonuclease activity (23). Thus, we determined whether inhibition of WRN catalytic activity was the result of oxidation of the polypeptide itself or of the DNA substrate. We performed oxidation reactions in the absence of WRN and then added aliquots to helicase and exonuclease assays in the presence of unoxidized WRN. As shown in Fig. 3*D*, neither helicase nor exonuclease activities were modulated. We conclude that iron-catalyzed oxidation inhibits helicase and exonuclease activities through direct oxidation of WRN itself.

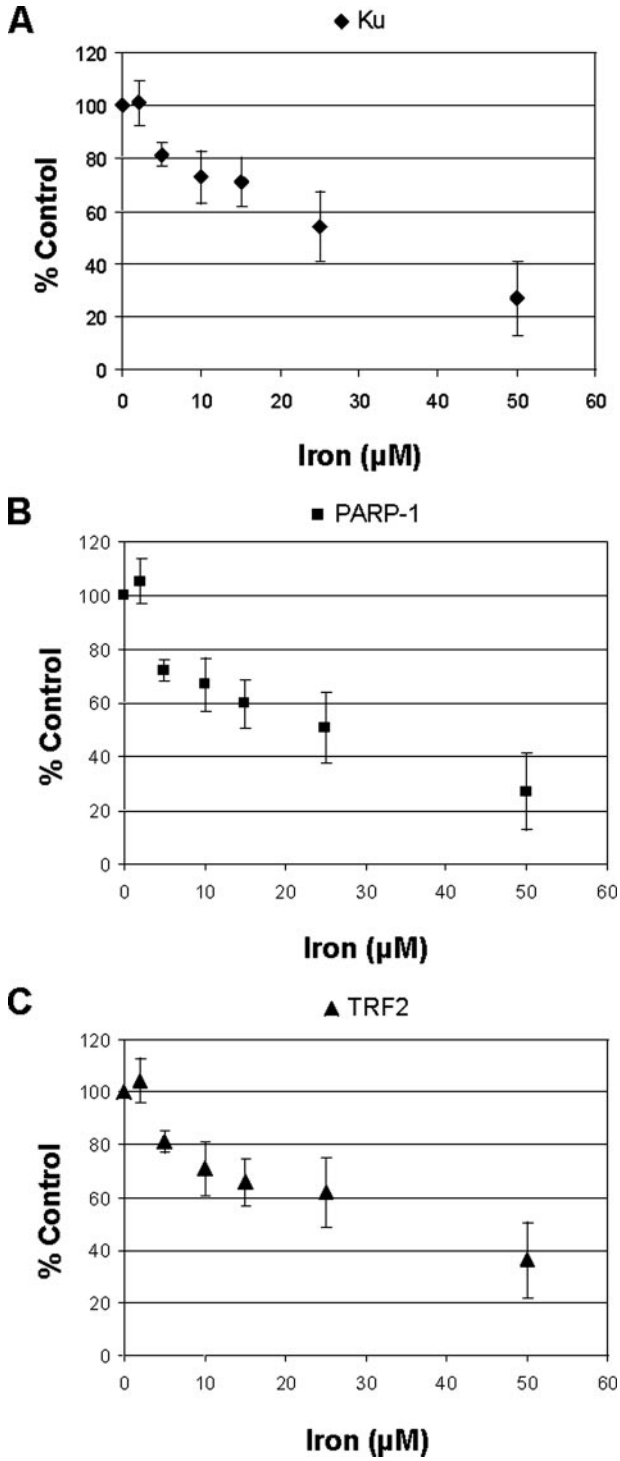

FIGURE 4. **Oxidation inhibits binding of WRN to its protein partners *in vitro*.** Wells were coated with the following purified recombinant proteins (500 fmol/well): Ku (*A*), PARP-1 (*B*), or TRF2 (*C*). After blocking with BSA, wells were incubated with recombinant WRN (500 fmol/well) from oxidation reactions (0–50 μM iron). Bound WRN was detected with anti-WRN antibodies followed by colorimetric analysis. Results represent the mean ± S.D. of three independent experiments.

Based on the inhibitory effects of oxidation on WRN catalytic activities, we next explored whether iron-mediated oxidation affects binding of WRN to its protein partners. We employed enzyme-linked immunosorbent assays to measure binding of WRN to Ku (Fig. 4*A*), PARP-1 (Fig. 4*B*), or TRF2 (Fig. 4*C*) fol-

lowing incubation in the absence or presence of increasing concentrations of iron. Incubation of WRN with 10 or 25 μM iron inhibited binding of WRN to protein partners ~25 and 50%, respectively (Fig. 4). Thus, oxidation of WRN in the presence of iron also inhibits binding of WRN to its protein partners.

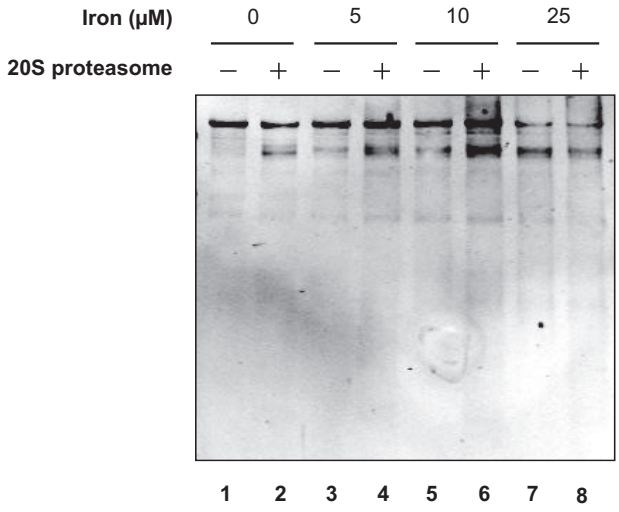

FIGURE 5. **Oxidized WRN is not degraded by the 20 S proteasome.** Recombinant WRN was incubated in the absence or presence of iron as indicated for 30 min at 37 °C. Subsequently, samples were incubated in the absence (*lanes 1*, *3*, *5*, and *7*) or presence (*lanes 2*, *4*, *6*, and *8*) of the 20 S proteasome for 1 h at 37 °C. Samples were run on SDS-PAGE, transferred to a polyvinylidene difluoride membrane, and blotted with anti-WRN antibodies. Results are representative of three independent experiments.

Protein oxidation typically perturbs the normal folding of the polypeptide. This misfolding may be recognized by the 20 S proteasome, which removes oxidatively modified proteins without ATP and without a requirement for ubiquitinylation (24). Thus, we measured the extent of WRN degradation by the 20 S proteasome following iron-mediated oxidation. Addition of the 20 S proteasome resulted in a slight degradation of WRN in the absence of iron (Fig. 5, *lanes 1* and *2*). However, incubation of WRN in the presence of increasing concentrations of iron and then subsequent incubation with the 20 S proteasome did not result in any further increased degradation (Fig. 5). Therefore, our results suggest that oxidized WRN is not targeted for degradation by the 20 S proteasome *in vitro*.

Next we sought to determine whether WRN is oxidized *in vivo* and whether increased oxidative stress results in accumulation of oxidatively modified protein. Therefore, we pretreated cells with the proteasome inhibitor MG-132. Subsequently, cells were exposed to H_2O_2. As shown in Fig. 6, both MG-132 and H_2O_2 treatment resulted in increased protein carbonyls, compared with untreated cells, as determined by anti-DNP antibodies (*Input*, *lower panels*). In addition, MG-132 or H_2O_2 treatment resulted in a lower molecular weight WRN species in immunoprecipitates compared with untreated cells (Fig. 6, *upper left panel*). Treatment of cells with MG-132 and H_2O_2 also resulted in a higher molecular weight WRN species in immunoprecipitates (Fig. 6, *upper left panel*). Furthermore, probing the WRN immunoprecipitates with anti-DNP antibodies resulted in increased protein carbonyl signals in samples exposed to MG-132 or H_2O_2 compared with untreated samples (Fig. 6, *lower left panel*). Thus, our results demonstrate that WRN can be modified oxidatively *in vivo* as determined by increased protein carbonyls following treatment of cells with H_2O_2 and proteasome inhibitor. Because purified 20 S proteasome did not initiate degradation of oxidatively modified WRN *in vitro*, other factors present *in vivo* are likely required. These could be an additional protease, a chaperone, or the regulatory cap present in the 26 S proteasome. The appearance of a lower molecular weight form of WRN following treatment with H_2O_2 or the proteasome inhibitor is consistent with a requirement for another protease to initiate degradation of WRN, as has been proposed for degradation of z-bands (25).

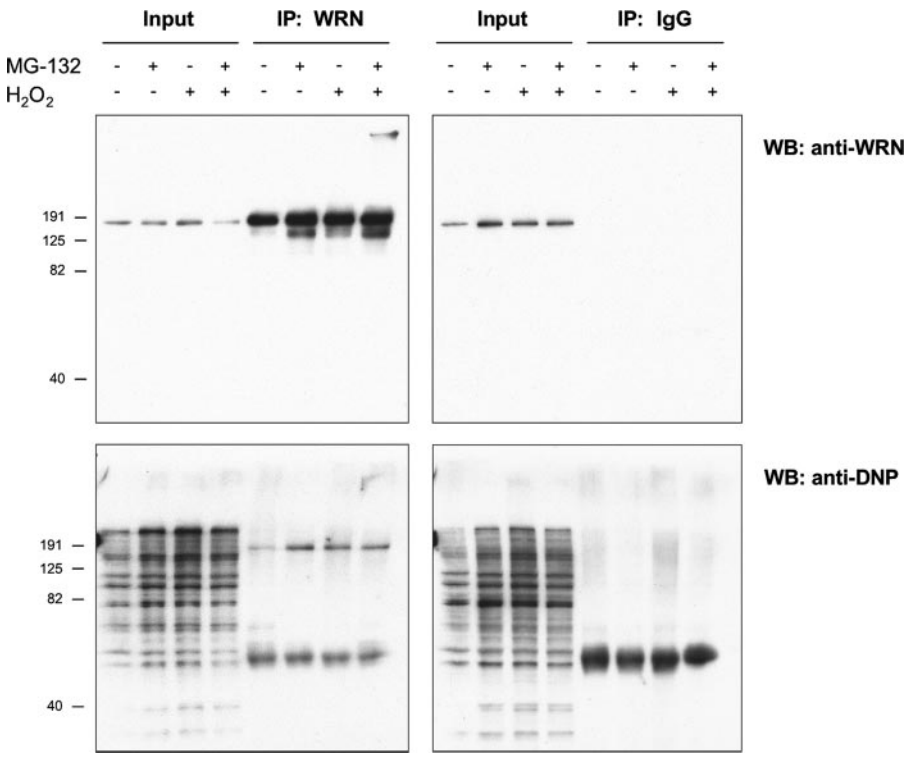

FIGURE 6. **WRN is oxidized *in vivo*.** HeLa cells were pretreated with MG-132 (20 μM) as indicated for 1 h. Subsequently, cells were incubated in the absence or presence of H_2O_2 (250 μM) as indicated for an additional 1 h. Whole cells extracts were prepared and incubated with either anti-WRN antibodies (*left panels*) or control IgG (*right panels*). Immunoprecipitates (*IP*) were analyzed by SDS-PAGE, and Western blotting (*WB*) was performed with anti-WRN (*upper panels*) or anti-DNP (*lower panels*) antibodies. Input is 2%. Molecular weight markers are indicated on the *left*. Results are representative of two independent experiments.

DISCUSSION

In this report we have demonstrated that WRN undergoes metal-catalyzed oxidation in a time- and concentration-dependent manner

in vitro. This reaction was mediated preferentially by iron, compared with copper. In addition, WRN was oxidized *in vivo* following exposure of cells to H_2O_2. Furthermore, we have shown that oxidative modification converts WRN to a form with impaired enzymatic activity and with impaired ability to participate in protein-protein interactions. Thus, cells that accumulate this post-translationally modified WRN could have functional defects similar to those observed in Werner syndrome patients, in which mutations in the *WRN* gene result in loss of WRN expression. Consistently, oxidative modification of fibrinogen has been shown previously to cause a functional impairment in clot formation akin to that seen in inherited dysfibrinogenemia (26).

WRN contains metal binding pockets within both ATPase/helicase and exonuclease motifs as mentioned previously. Thus, the specificity of the oxidative modification of WRN is understandable as metal-catalyzed oxidation is not a random event. It is site-specific as a consequence of the binding of divalent cations to metal binding site(s) within proteins (1, 27). Choudhary *et al.* (28) found that iron and copper very effectively inhibited WRN helicase activity compared with other metals at the same concentration (10 μM). In addition, iron was more effective than copper in inhibiting WRN unwinding reactions at even lower concentrations. Consistently, we observed that iron-catalyzed oxidation of WRN resulted in inhibition of ATPase, helicase, and exonuclease activities to various extents. The relative preservation of WRN ATPase activity in the presence of iron is not surprising because the reaction it catalyzes is only one component of the overall helicase reaction. For WRN helicase and exonuclease activities, it may be that a greater fraction of helicase activity is lost compared with exonuclease activity at low iron concentrations. For example, in the presence of 10 μM iron, WRN helicase activity was inhibited 61%, whereas exonuclease activity was inhibited 46% (Fig. 3, *A* and *C*). The potential physiological or regulatory significance of such differential inhibition as a result of oxidation remains to be determined. Taken together, our observations that iron was more effective than copper in oxidizing WRN *in vitro*, and that iron-catalyzed oxidation of WRN resulted in decreased helicase and exonuclease activities, and the greater abundance and availability of intracellular iron, suggest that WRN is likely oxidized by iron *in vivo* and this oxidation will result in inhibition of the enzymatic activities of WRN. Similarly, mitochondrial DNA polymerase γ has been shown to be oxidized *in vitro* and *in vivo* (29). Oxidation of the catalytic subunit of DNA polymerase γ resulted in decreased polymerase activity, which may lead to decreased mitochondrial DNA replication and repair capabilities.

As WRN has been suggested to participate in DNA replication, recombination, repair, and telomere maintenance, metal-catalyzed oxidation may inhibit the role of WRN in these processes, leading to genome instability. For example, WRN has been shown to physically interact with Ku (30), and this interaction stimulates WRN exonuclease activity (30–32). The participation of Ku in the repair of DNA double strand breaks suggests that WRN may be important for DNA end processing during repair events. Ku has also been localized to telomeres (33), and the interaction between Ku and WRN may be important for telomere maintenance. Similarly, WRN has been shown to interact physically with the telomere repeat-binding protein TRF2, and TRF2 stimulates WRN helicase activity, lending further support to a role for WRN at telomeres (18). WRN also physically interacts with PARP-1 (21). In addition, Werner syndrome cells are deficient in the PARP-1 poly-(ADP-ribosyl)ation pathway after oxidative stress (21), suggesting a role for WRN in repair of oxidative DNA damage. Iron-mediated oxidation of WRN resulted in decreased binding to its protein partners, Ku, TRF2, and PARP-1, suggesting that oxidatively modified WRN may have deleterious effects on DNA repair and telomere maintenance pathways.

In yeast, aging is accompanied by increased genome instability, for example in the form of loss of heterozygosity (34). Age-induced loss of heterozygosity may result from an age-dependent increase in DNA double strand breaks and/or a decrease in the repair of such breaks (34). As oxidized proteins accumulate preferentially in old yeast cells (35), it is possible that old cells accumulate damaged proteins, resulting in decreased DNA repair (36). Our results presented here suggest that oxidatively modified WRN is refractory to degradation by the proteasome. Thus, increased oxidative stress in old cells may result in increased WRN oxidation and accumulation of catalytically inactive pools of WRN, promoting inefficient DNA repair and genome instability.

Although Werner syndrome is clinically notable for its phenotype of premature aging, cells from patients with Werner syndrome were shown to carry an increased burden of oxidatively damaged proteins well before WRN was recognized to be a DNA helicase and exonuclease (10, 37, 38). Recently, Werner syndrome patients were also shown to have elevated levels of oxidative stress parameters (39), providing additional evidence of an *in vivo* prooxidant state. As in Werner syndrome, tissues from mice lacking *ATM* (ataxia-telangiectasia mutated) are also under oxidative stress (40). ATM is a protein kinase that becomes activated following the formation of double-stranded DNA breaks. The mechanisms by which a defective response to DNA damage leads to oxidative stress are unknown, as are the mechanisms by which oxidative stress increases during aging. However, the ability of oxidative stress to inactivate DNA repair enzymes such as WRN could give rise to a self-amplifying "vicious cycle." Oxidative inactivation of a fraction of WRN could thus increase oxidative stress, driving the cycle at an increasingly accelerated rate.

Acknowledgments—We thank Nancy Wehr for excellent technical assistance and Drs. Heng Kuan Wong and Meltem Muftuoglu for critical reading of the manuscript.

REFERENCES

1. Levine, R. L., and Stadtman, E. R. (2001) *Exp. Gerontol.* **36,** 1495–1502
2. Stadtman, E. R., and Berlett, B. S. (1998) *Drug Metab. Rev.* **30,** 225–243
3. Meneghini, R. (1997) *Free Radic. Biol. Med.* **23,** 783–792
4. Sandstrom, B. E., Granstrom, M., and Marklund, S. L. (1994) *Free Radic. Biol. Med.* **16,** 177–185
5. Mello-Filho, A. C., and Meneghini, R. (1991) *Mutat. Res.* **251,** 109–113
6. Stadtman, E. R. (1990) *Free Radic. Biol. Med.* **9,** 315–325
7. Fucci, L., Oliver, C. N., Coon, M. J., and Stadtman, E. R. (1983) *Proc. Natl.*

Acad. Sci. U. S. A. **80,** 1521–1525
8. Stadtman, E. R., and Levine, R. L. (2000) *Ann. N. Y. Acad. Sci.* **899,** 191–208
9. Epstein, C. J., Martin, G. M., Schultz, A. L., and Motulsky, A. G. (1966) *Medicine* (*Baltimore*) **45,** 177–221
10. Oliver, C. N., Ahn, B. W., Moerman, E. J., Goldstein, S., and Stadtman, E. R. (1987) *J. Biol. Chem.* **262,** 5488–5491
11. Caruthers, J. M., and McKay, D. B. (2002) *Curr. Opin. Struct. Biol.* **12,** 123–133
12. Tuteja, N., and Tuteja, R. (2004) *Eur. J. Biochem.* **271,** 1849–1863
13. Fry, D. C., Chubby, S. A., and Mildvan, A. S. (1986) *Proc. Natl. Acad. Sci. U. S. A.* **83,** 907–911
14. Mian, I. S. (1997) *Nucleic Acids Res.* **25,** 3187–3195
15. Perry, J. J., Yannone, S. M., Holden, L. G., Hitomi, C., Asaithamby, A., Han, S., Cooper, P. K., Chen, D. J., and Tainer, J. A. (2006) *Nat. Struct. Mol. Biol.* **13,** 414–422
16. Mushegian, A. R., Bassett, D. E., Jr., Boguski, M. S., Bork, P., and Koonin, E. V. (1997) *Proc. Natl. Acad. Sci. U. S. A.* **94,** 5831–5836
17. Orren, D. K., Brosh, R. M., Jr., Nehlin, J. O., Machwe, A., Gray, M. D., and Bohr, V. A. (1999) *Nucleic Acids Res.* **27,** 3557–3566
18. Opresko, P. L., von Kobbe, C., Laine, J. P., Harrigan, J., Hickson, I. D., and Bohr, V. A. (2002) *J. Biol. Chem.* **277,** 41110–41119
19. Di Noto, L., Whitson, L. J., Cao, X., Hart, P. J., and Levine, R. L. (2005) *J. Biol. Chem.* **280,** 39907–39913
20. Luo, S., Wehr, N. B., and Levine, R. L. (2006) *Anal. Biochem.* **350,** 233–238
21. von Kobbe, C., Harrigan, J. A., May, A., Opresko, P. L., Dawut, L., Cheng, W. H., and Bohr, V. A. (2003) *Mol. Cell. Biol.* **23,** 8601–8613
22. Bernstein, D. A., Zittel, M. C., and Keck, J. L. (2003) *EMBO J.* **22,** 4910–4921
23. Machwe, A., Ganunis, R., Bohr, V. A., and Orren, D. K. (2000) *Nucleic Acids Res.* **28,** 2762–2770
24. Grune, T., Merker, K., Sandig, G., and Davies, K. J. (2003) *Biochem. Biophys. Res. Commun.* **305,** 709–718
25. Williams, A. B., Courten-Myers, G. M., Fischer, J. E., Luo, G., Sun, X., and Hasselgren, P. O. (1999) *FASEB J.* **13,** 1435–1443
26. Shacter, E., Williams, J. A., and Levine, R. L. (1995) *Free Radic. Biol. Med.* **18,** 815–821
27. Farber, J. M., and Levine, R. L. (1986) *J. Biol. Chem.* **261,** 4574–4578
28. Choudhary, S., Sommers, J. A., and Brosh, R. M., Jr. (2004) *J. Biol. Chem.* **279,** 34603–34613
29. Graziewicz, M. A., Day, B. J., and Copeland, W. C. (2002) *Nucleic Acids Res.* **30,** 2817–2824
30. Cooper, M. P., Machwe, A., Orren, D. K., Brosh, R. M., Ramsden, D., and Bohr, V. A. (2000) *Genes Dev.* **14,** 907–912
31. Karmakar, P., Snowden, C. M., Ramsden, D. A., and Bohr, V. A. (2002) *Nucleic Acids Res.* **30,** 3583–3591
32. Li, B., and Comai, L. (2001) *J. Biol. Chem.* **276,** 9896–9902
33. Featherstone, C., and Jackson, S. P. (1999) *Mutat. Res.* **434,** 3–15
34. McMurray, M. A., and Gottschling, D. E. (2003) *Science* **301,** 1908–1911
35. Aguilaniu, H., Gustafsson, L., Rigoulet, M., and Nystrom, T. (2003) *Science* **299,** 1751–1753
36. Sinclair, D. A. (2003) *Science* **301,** 1859–1860
37. Gray, M. D., Shen, J. C., Kamath-Loeb, A. S., Blank, A., Sopher, B. L., Martin, G. M., Oshima, J., and Loeb, L. A. (1997) *Nat. Genet.* **17,** 100–103
38. Shen, J. C., Gray, M. D., Oshima, J., Kamath-Loeb, A. S., Fry, M., and Loeb, L. A. (1998) *J. Biol. Chem.* **273,** 34139–34144
39. Pagano, G., Zatterale, A., Degan, P., d'Ischia, M., Kelly, F. J., Pallardo, F. V., Calzone, R., Castello, G., Dunster, C., Giudice, A., Kilinc, Y., Lloret, A., Manini, P., Masella, R., Vuttariello, E., and Warnau, M. (2005) *Free Radic. Res.* **39,** 529–533
40. Barlow, C., Dennery, P. A., Shigenaga, M. K., Smith, M. A., Morrow, J. D., Roberts, L. J., Wynshaw-Boris, A., and Levine, R. L. (1999) *Proc. Natl. Acad. Sci. U. S. A.* **96,** 9915–9919